



The background features a large, faint number '6' in the upper right quadrant. The rest of the page is filled with various abstract geometric shapes, including rectangles, triangles, and rounded forms, in shades of light gray and white, creating a layered, architectural feel.

6

**SUMMARY, DISCUSSION  
AND FUTURE PERSPECTIVES**

This thesis presents the potential of radioimmunoscinigraphy (RIS) and radioimmunotherapy (RIT) in clinical studies in patients diagnosed with head and neck squamous cell carcinoma (HNSCC). Squamous cell carcinoma is the most frequently occurring malignant tumor in the head and neck and originates predominantly (>95%) in the oral cavity, pharynx, and the larynx. The estimated worldwide incidence of HNSCC in 2002 was more than 563,000 cases, and more than 301,000 deaths were reported (1). All studies described in this thesis, were conducted with monoclonal antibodies (MAbs) directed against CD44v6, a target antigen abundantly expressed in HNSCC.

In the introduction (**Chapter 1**) of this thesis, an overview is given of current diagnostic modalities and therapies of HNSCC, while the possibilities, requirements, and restrictions of RIS and RIT in HNSCC are discussed. Studies using MAbs directed against HNSCC-associated antigens, such as CD44v6, are dealt with in more detail. Finally, novel diagnostic and treatment strategies using radiolabeled MAbs are discussed.

One of the limitations encountered in previous RIT studies using chimeric MAbs (cMAbs) directed against CD44v6 in patients is immunogenicity. Development of human antibody responses can lead to allergic reactions like anaphylaxis, and may lead to rapid clearance of the MAb, especially when the MAb is administered repeatedly. In case of RIT this will result in less dose deposition in the tumor. **Chapter 2** presents the results of a phase I radiation dose-escalation RIT study in HNSCC patients using the anti-CD44v6 humanized MAb bivatuzumab, also called BIWA 4, labeled with rhenium-186 ( $^{186}\text{Re}$ ). In this study, the safety, maximum tolerable dose (MTD), immunogenicity, and therapeutic potential of the radioimmunoconjugate was determined in 20 patients with incurable recurrent and/or metastatic HNSCC. All patients received a single dose of  $^{186}\text{Re}$ -bivatuzumab in dose-escalation steps of 0.74, 1.11, 1.48, 1.85, and 2.22 GBq/m<sup>2</sup>. The MTD was established at 1.85 GBq/m<sup>2</sup> at which level dose-limiting myelotoxicity was seen in 1 out of 6 patients. Three patients received a second dose of 1.85 GBq/m<sup>2</sup> at least 3 months after the first dose. First and second administrations were all well tolerated and targeting of tumor lesions proved to be consistently very good, as shown by planar and tomographic images of the head and neck. Figure 1 shows typical whole-body  $\gamma$ -camera images of a patient with HNSCC who received  $^{186}\text{Re}$ -labeled anti-CD44v6 MAb. The only significant manifestations of toxicity were dose-limiting myelotoxicity consisting of thrombo- and leukocytopenia. CTC grade 4 myelotoxicity was seen in 2 patients treated at the dose level 2.22 GBq/m<sup>2</sup>. To a lesser extent oral mucositis was observed, CTC grade 2 in 2 out of 6 patients who received 1.85 GBq/m<sup>2</sup> and in 3 out of 5 patients who received 2.22 GBq/m<sup>2</sup>. Two of the 3 patients who underwent a second administration showed oral mucositis after both

administrations. After the second administration, oral mucositis showed no increase in severity, compared with the first administration. All patients in the study population had been treated previously with external beam irradiation, which had caused severe mucositis in some of the patients. It is possible that this prior treatment could aggravate the mucositis encountered after RIT.

One patient treated at the 1.11 GBq/m<sup>2</sup> dose level was admitted to the hospital because of unexplained seizures 5 days after start of RIT. During hospitalization, angioedema caused reversible respiratory distress 8 days after start of RIT. Eleven days after start of RIT the patient was dismissed from the hospital. She was found dead at home 22 days after RIT. Upon examination, no relationship between antibody administration and death could be found, but the possibility of a relationship could not be excluded. No human anti-bivatuzumab response (HAHA) was detected after analysis of serum from this patient.

Stable disease, lasting 6 to 21 weeks, was observed in 3 out of 6 patients treated at MTD-level. Regarding the immunogenicity, only 2 out of 20 (10%) patients experienced a HAHA, whereas RIT studies with the anti-CD44v6 cMab U36 in HNSCC patients showed a human anti-U36 response (HACA) in 5 out of 12 (42%) patients (2). Moreover, in 3 radioimmunoscinigraphy-biodistribution studies performed with <sup>99m</sup>Tc-bivatuzumab in a total of 28 patients with HNSCC (n=10), non-small-cell lung cancer (n=9), and breast cancer (n=9), no HAHA responses were observed (3,4). It was concluded that <sup>186</sup>Re-bivatuzumab can be safely administered, also when injected twice.

The observation of antitumor effects in patients with bulky disease, offers opportunities for further development of RIT with single or multiple doses of <sup>186</sup>Re-labeled bivatuzumab. Although no objective responses were achieved in patients with incurable HNSCC, one might expect a much better performance of this radioimmunoconjugate in an adjuvant setting shortly after surgery in patients with minimal residual disease and therefore at risk for development of distant metastasis. The fact that the uptake of MAbs is higher in small volume HNSCC tumors (1 cm<sup>3</sup>) as compared to large volume HNSCC tumors (50 cm<sup>3</sup>), supports further development of RIT as an option for adjuvant targeted therapy of minimal residual HNSCC (5). Another possibility to improve RIT efficacy is by decreasing bone marrow toxicity using autologous blood or bone marrow progenitor cell transplantation. A previous RIT study in HNSCC showed that re-infusion of granulocyte colony-stimulating factor stimulated unprocessed whole blood, makes it possible to increase the MTD, and possibly enhancing antitumor effects (6). Enhancement of the efficacy of RIT may also be established by combining RIT with targeted therapies that have no or low myelotoxicity. On the analogy of approaches in which anti-EGFR antibodies are combined with external beam irradiation, as used for treatment of locally advanced HNSCC (7), anti-EGFR

MAbs might also be combined with RIT. Indeed, combination of RIT with EGFR blocking MAb 425 in a preclinical trial with HNSCC xenograft bearing nude mice, showed an additional effect (8).

The data acquired from the phase I radiation dose-escalation RIT study with  $^{186}\text{Re}$ -bivatuzumab in HNSCC patients, were also used for dosimetric analysis, as described in **Chapter 3**. Whole body scintigraphy was used to draw regions around sites or organs of interest. Residence times in these organs and sites were calculated and entered into the MIRDOSE3 program, to obtain absorbed doses in all source organs except for the red marrow. The red marrow dose was calculated with a blood-derived method (9). Twenty-one studies in 18 patients were used for dosimetric analysis, 5 of them in women and 16 in men. The data acquired from a second dose of  $1.85 \text{ GBq/m}^2$  administered to 3 patients at least 3 months after the first dose are included in these 21 studies. The mean red marrow dose was  $0.49 \pm 0.03 \text{ mGy/MBq}$  in men and  $0.64 \pm 0.03 \text{ mGy/MBq}$  in women. The normal organ with the highest absorbed doses appeared to be the kidneys (mean dose in men  $1.61 \pm 0.75 \text{ mGy/MBq}$ ; mean dose in women  $2.15 \pm 0.95 \text{ mGy/MBq}$ ; maximum dose of kidneys in all patients 11 Gy) and are not expected to lead to renal toxicity. The doses delivered to the tumor, recalculated to the MTD level of  $1.85 \text{ GBq/m}^2$ , ranged from 3.8-76.4 Gy, with a median of 12.4 Gy. A strong correlation ( $r = -0.79$ ) was found between the amount of radioactivity per kg body weight and platelet and white blood cell nadir, respectively.

In conclusion, RIT with  $^{186}\text{Re}$ -bivatuzumab is safe, and has a low immunogenicity, allowing repeated administration. The only toxicity observed in this study was myelotoxicity caused by circulating radioimmunoconjugate and, in some patients, mild oral mucositis. Dosimetric analysis showed that this treatment is also safe with respect to absorbed doses to normal organs. At the highest RIT dose levels, antitumor effects have been observed consistently, although higher tumor absorbed doses (>60 Gy) should be achieved before objective responses might be expected from RIT monotherapy.

Selective tumor targeting by bivatuzumab as demonstrated in the RIT studies, has also stimulated the use of this MAb in other therapeutic approaches. Despite promising initial results, the large scale use of radioimmunoconjugates may encounter problems related to logistics and radiation safety. Omission of radioactivity could solve these issues, and therefore, an anti-CD44v6 antibody-drug conjugate designated bivatuzumab mertansine was developed by the sponsor of the bivatuzumab RIT trial. Antibody-drug conjugates are particularly attractive, because no bone marrow toxicity has to be expected, and therefore perspectives might arise for combined treatment with conventional chemotherapeutics.

Bivatuzumab mertansine is a tumor-activated prodrug conjugate, which

consists of the super-toxic anti-microtubule drug mertansine (DM1) covalently linked to bivatuzumab. After binding to CD44v6, the complex can be internalized, and the mertansine molecules will be released intracellularly by cleavage of the antibody-mertansine disulfide bonds. In a study with HNSCC patients described by Tjink et al. (10), the safety, MTD, and preliminary efficacy of bivatuzumab mertansine were assessed, and the pharmacokinetics and immunogenicity were determined after 3 weekly i.v. injections of the conjugate. In this study, no toxicity related to free mertansine as a result of deconjugation in the circulation was observed, and no evidence was found for the non-specific uptake by cells not expressing the antigen. The main toxicity of bivatuzumab mertansine was directed against the skin, most probably due to CD44v6 expression in this tissue (cross-reactivity). The majority of skin reactions was reversible, however, one fatal drug-related adverse event occurred. Toxic epidermal necrolysis appeared in 1 patient treated at a dose of 140 mg/m<sup>2</sup>. Toxicity was most probably triggered by the cross-reactivity of bivatuzumab with skin keratinocytes. There was no evidence for a dose-toxicity relationship, and it is therefore difficult to predict when severe skin toxicity will occur. It was decided to discontinue further clinical development of bivatuzumab mertansine. From this study and parallel studies with bivatuzumab mertansine, it can be concluded that strict tumor-selective expression of the particular target antigen is required, when using supertoxic antibody-drug conjugates for therapy. The expression of CD44v6 was probably not selective enough to allow safe therapy. This conclusion is probably reasonable for approaches in which supertoxic drugs like mertansine are used, but may not necessarily be the case for other approaches like RIT. In 3 RIT trials with <sup>186</sup>Re-labeled anti-CD44v6 MAbs U36 and bivatuzumab in a total of 45 administrations (2,6,11), only 1 patient developed reversible skin reactions 8 days after the start of RIT, consisting of angioedema (CTC grade 3) and rash (CTC grade 3). This difference in toxicity between CD44v6-specific RIT (<sup>186</sup>Re) conjugates and CD44v6-specific mertansine conjugates can be explained by the two following aspects. First, radiation deposition with <sup>186</sup>Re is relatively slow due to the long half-life of 89 hours of this  $\beta$ -emitting radionuclide. Second, whereas the energy and path length (5 mm) of the  $\beta$ -emission of <sup>186</sup>Re are ideal for irradiation of small-sized to medium-sized tumors (0.5-1 cm) (12), toxicity in the skin is just moderate due to the fact that a large part of the disintegration energy dissipates outside the distribution volume of this tissue (especially the basal cell layer). This explains low skin toxicity in the case of RIT.

Aforementioned studies illustrate that selective targeting of tumors by targeted therapies like MAbs is possible, and that MAb imaging might be a valuable tool to visualize and quantify uptake of the MAb in tumor and normal organs. For this purpose the use of  $\gamma$ -camera images can be very informative, although there is still room for improvements as illustrated by Figure 1. For

example, the images shown in Figure 1 did not provide much details of organs. The fact that the tumor looked much larger than in reality, has also to do with limited resolution. No anatomical details are visible. Most importantly, a need for more accurate quantification was felt, a reason to explore the potential of positron emission tomography (PET) for MAb imaging.

**Chapter 4** evaluates immuno-PET, the combination of PET with MABs, as an option to improve tumor detection and to guide MAb-based therapy. The long-lived positron emitter zirconium-89 ( $^{89}\text{Zr}$ ) has ideal physical characteristics for immuno-PET with intact MABs, but was never used before in a clinical setting. In a phase I study presented in this thesis, the diagnostic imaging performance of immuno-PET with  $^{89}\text{Zr}$ -labeled-chimeric anti-CD44v6 MAb (cMAb) U36 was evaluated in 20 patients with HNSCC, who were at high risk of having neck lymph node metastases and therefore were scheduled to undergo neck dissection with or without resection of the primary tumor. All patients received 75 MBq  $^{89}\text{Zr}$ -cMAb U36. All patients were examined by computerized tomography (CT) and/or magnetic resonance imaging (MRI) and immuno-PET prior to surgery. Six patients also underwent PET with  $^{18}\text{F}$ -fluoro-2-deoxy-D-glucose (FDG-PET). Immuno-PET scans were acquired up to 144 hours after injection. Diagnostic findings were recorded per neck side (left or right) as well as per lymph node level (6 levels per side), and compared with histopathological outcome. Immuno-PET detected all primary tumors ( $n = 17$ ) as well as lymph node metastases in 18 of 25 positive levels (sensitivity 72%) and in 11 of 15 positive sides (sensitivity 73%). Interpretation of immuno-PET was correct in 112 of 121 operated levels (accuracy 93%) and in 19 of 25 operated sides (accuracy 76%). As illustrated in Figure 2,  $^{89}\text{Zr}$  immuno-PET images show much more detail of the organs and tumor, compared with the  $\gamma$ -camera images in Figure 1. For CT/MRI sensitivities of 60% and 73% and accuracies of 90% and 80% were found per level and side, respectively. In the 6 patients with 7 tumor involved neck levels and sides, immuno-PET and FDG-PET gave comparable diagnostic results. In this study, immuno-PET with  $^{89}\text{Zr}$ -cMAb U36 performed at least as good as CT/MRI for detection of HNSCC lymph node metastases. The future application of PET/CT might further support image interpretation.

The data acquired from the phase I immuno-PET study with  $^{89}\text{Zr}$ -labeled-cMAb U36 in HNSCC patients were also used for dosimetric and safety analysis, as described in **Chapter 5**. Biodistribution of the radioimmunoconjugate was evaluated by radioactivity measurement in blood, red marrow, and in biopsies from the surgical specimen obtained 168 hours after injection. Uptake of the radioimmunoconjugate in tumors and organs of interest was quantified by creating volumes of interest in the immuno-PET images. Residence times in tumors and organs were calculated and entered into the OLINDA/EXM 1.0

program, to obtain absorbed doses. The red marrow dose was calculated using a blood-derived method (13). Injection of  $^{89}\text{Zr}$ -cMAb U36 was well tolerated in all subjects, with no serious or drug-related adverse events reported. Two patients developed a HACA response, but this did not affect the body clearance of the radioimmunoconjugate. Quantification of blood-pool activity in the left ventricle of the heart showed good agreement with the activity measured in blood samples (difference equals  $0.2\% \pm 16.9\%$  [mean  $\pm$  SD]), except for heavy weight patients ( $>100$  kg). The mean red marrow dose was  $0.07 \pm 0.02$  mSv/MBq in men and  $0.09 \pm 0.01$  mSv/MBq in women. The normal organ with the highest absorbed dose was the liver (mean dose in men  $96.49 \pm 21.02$  mSv; in women  $105.26 \pm 16.25$  mSv), and thereafter followed by kidneys, thyroid, lungs and spleen. The mean effective dose was  $0.53 \pm 0.03$  mSv/MBq in men and  $0.66 \pm 0.03$  mSv/MBq in women. Excretion via the urinary pathway was low with a mean excretion of  $2.59 \pm 1.89$  %ID  $^{89}\text{Zr}$  during the first 72 h after injection. The mean effective dose for the whole body was  $0.53 \pm 0.03$  mSv/MBq in men and  $0.66 \pm 0.03$  mSv/MBq in women. Evaluation of quantification of MAb uptake in tumors showed a good agreement between %ID/g derived from biopsy data 168 h after injection and PET data 144 h after injection, with slightly lower values for PET (mean deviation,  $-8.4\% \pm 34.5\%$ ).

In conclusion, the results of the first-in-human immuno-PET study with  $^{89}\text{Zr}$  labeled cMAb U36 in HNSCC patients, showed that  $^{89}\text{Zr}$  immuno-PET performs at least as good as CT and MRI in detection of primary tumor and lymph node metastases. In general,  $^{89}\text{Zr}$  immuno-PET is a new, noninvasive diagnostic modality, and more important, a promising quantitative imaging tool which can be broadly applied in MAb research e.g. for the selection of high potential candidate MABs for therapy as well as of patients most likely to benefit from specific MAB treatment.

Despite clinical optimism, it is fair to state that the efficacy of most of the current FDA approved MABs is still limited, with benefit for just a portion of patients. Moreover, the costs of MAB therapy are excessive. The question is how to improve the efficacy of MAB-based therapy and how to identify patients with the highest chance of benefit. In other words: when, how, and for whom should antibody-based therapy be reserved? We foresee that quantitative imaging of MABs by immuno-PET can be a valuable tool at several stages of MAB development and application. From first-in-human clinical trials with new MABs, it is important to learn about the ideal MAB dosing for optimal tumor targeting (e.g., saturation of receptors), the uptake in critical normal organs to anticipate toxicity (although immuno-PET had not predicted skin toxicity caused by bivatuzumab mertansine targeting), and the interpatient variations in pharmacokinetics and tumor targeting. MAB imaging might



provide this information in an efficient and safe way, with fewer patients treated at suboptimal doses. This approach is especially attractive when the MAb of interest is directed against a novel tumor target that has not been validated in clinical trials before. Quantitative MAb imaging might also be of value to guide the optimal use of FDA-approved MAbs. In current practice, tissue analyses are often performed to confirm target expression and to select patients for MAb therapy. For example, patients with metastatic breast cancer are only eligible for therapy with the anti-human epidermal growth factor receptor-2 (HER2) MAb trastuzumab when protein overexpression or gene amplification has been confirmed on a biopsy of the tumor by immunohistochemistry or fluorescence in situ hybridization (in 20% - 30% of patients). It is questionable, however, whether a representative overview of *in vivo* HER2 expression status can be obtained by analysis of just one single biopsy, whereas the expression of an antigen can be heterogenous within a single tumor and can also differ between primary tumor and metastases. Pretherapy imaging might have added value for patient selection, because it can be used to assess target expression and MAb accumulation in all tumor lesions and normal tissues, noninvasively, quantitatively, and even over time (four-dimensional). This information might be particularly relevant when MAb therapy is combined with other treatment modalities like chemo- and radiotherapy, to find routes to maximum synergism. Ideally, topographic information on tumor extension is obtained to enable assessment of homogeneity of MAb tumor accumulation. Until now, pretherapy antibody imaging has mostly been applied as a prelude to RIT for assessment of dosimetry (14). In this setting, quantitative imaging is particularly attractive because of the small therapeutic window of RIT, with bone marrow toxicity being dose limiting.

On the basis of the encouraging findings with immuno-PET described herein, several clinical trials with  $^{89}\text{Zr}$ -labeled mAbs were recently started, among which is a study with  $^{89}\text{Zr}$ -trastuzumab for the assessment of HER2 expression status and for detection of HER2-positive tumor lesions in breast cancer patients. Preliminary results from the first patients in this study (15) showed excellent tumor tracer uptake and a resolution that was much better than that observed in previous SPECT studies with  $^{111}\text{In}$ -trastuzumab (16). In other immuno-PET studies,  $^{89}\text{Zr}$ -labeled bevacizumab, cetuximab and ibritumomab tiuxetan, respectively, showed promising results when applied as a tool for non-invasive evaluation of MAb uptake and treatment planning (17,18,19). It is to be expected that more studies will follow, also in patients with HNSCC, in this interesting field of research.

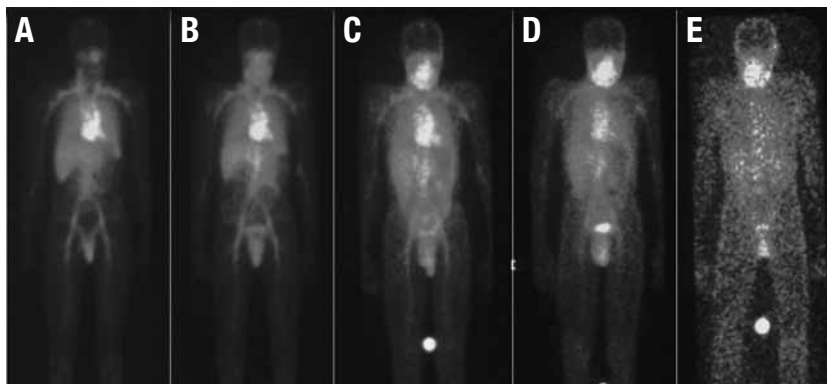


**FIGURE 1.**

Planar whole body scans of a patient with a tumor in the right oropharynx. Scans were acquired 1 (A), 24 (B), 72 (C), 144 (D), and 312 (E) hours after administration of  $^{186}\text{Re}$ -labeled cMAb U36. Immediately after injection, the MAb resides in the blood pool. Relative uptake of the radioimmunoconjugate in the tumor increases over time, while the tumor becomes better delineated as background activity decreases.

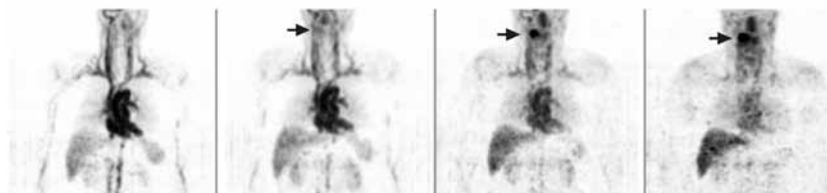


**FIGURE 2.**

Representative coronal images of male patient with oropharyngeal tumor (indicated by arrows), arranged (left to right) from 1, 24, 72, and 144 h after injection, showing circulating  $^{89}\text{Zr}$ -cmAb U36 in heart, uptake in organs and increased uptake in time of  $^{89}\text{Zr}$ -cmAb U36 in tumor.

## REFERENCES

1. Parkin DM, Bray F, Ferlay J, Pisani P. Global cancer statistics, 2002. *CA Cancer J Clin* 2005;55:74-108.
2. Colnot DR, Quak JJ, Roos JC, van Lingen A, Wilhelm AJ, van Kamp GJ, et al. Phase I therapy study of  $^{186}\text{Re}$ -labeled chimeric monoclonal antibody U36 in patients with squamous cell carcinoma of the head and neck. *J Nucl Med* 2000;41:1999-2010.
3. Colnot DR, Roos JC, de Bree R, Wilhelm AJ, Kummer JA, Hanft G, et al. Safety, biodistribution, pharmacokinetics, and immunogenicity of  $^{99\text{m}}\text{Tc}$ -labeled humanized monoclonal antibody BIWA 4 (bivatuzumab) in patients with squamous cell carcinoma of the head and neck. *Cancer Immunol Immunother* 2003;52:576-582.
4. Koppe MJ, Schaijk FG, Roos JC, Leeuwen P, Heider KH, Kuthan H, et al. Safety, pharmacokinetics, immunogenicity, and biodistribution of  $^{186}\text{Re}$ -labeled humanized monoclonal antibody BIWA 4 (bivatuzumab) in patients with early-stage breast cancer. *Cancer Biother Radiopharm* 2004;19:720-729.
5. de Bree R, Kuik DJ, Quak JJ, Roos JC, van den Brekel MWM, Castelijns JA, et al. The impact of tumour volume and other characteristics on uptake of radiolabeled monoclonal antibodies in tumour tissue of head and neck cancer patients. *Eur J Nucl Med* 1998;25:1562-1565.
6. Colnot DR, Ossenkoppele GJ, Roos JC, Quak JJ, de Bree R, Börjesson PKE, et al. Reinfusion of unprocessed, granulocyte colony-stimulating factor-stimulated whole blood allows dose escalation of  $^{186}\text{Re}$ -labeled chimeric monoclonal antibody U36 radioimmunotherapy in a phase I dose escalation study. *Clin Cancer Res* 2002;8:3401-3406.
7. Bonner JA, Harari PM, Giralt J, Azarnia N, Shin DM, Cohen RB, et al. Radiotherapy plus cetuximab for squamous-cell carcinoma of the head and neck. *N Engl J Med* 2006;354:567-578.
8. van Gog FB, Brakenhoff RH, Stigter-van Walsum M, Snow GB, van Dongen GAMS. Perspectives of combined radioimmunotherapy and anti-EGFR antibody therapy for the treatment of residual head and neck cancer. *Int J Cancer* 1998;77:13-18.
9. Shen S, DeNardo GL, Sgouros G, O'Donnell RT, DeNardo SJ. Practical determination of patient-specific marrow dose using radioactivity concentration in blood and body. *J Nucl Med* 1999;40:2102-2106.
10. Tjink BM, Buter J, de Bree R, Giaccone G, Lang MS, Staab A, et al. A phase I dose escalation study with anti-CD44v6 bivatuzumab mertansine in patients with incurable squamous cell carcinoma of the head and neck or esophagus. *Clin Cancer Res* 2006;12:6064-6072.
11. Börjesson PKE, Postema EJ, Roos JC, Colnot DR, Marres HA, van Schie MH, et al. Phase I therapy study with  $^{186}\text{Re}$ -labeled humanized monoclonal antibody BIWA 4 (bivatuzumab) in patients with head and neck squamous cell carcinoma. *Clin Cancer Res* 2003;9:3961S-3972S.

12. Wessels BW, Rogus RD. Radionuclide selection and model absorbed dose calculations for radiolabeled tumor associated antibodies. *Med Phys* 1984;11:638-645.
13. Sgouros G. Bone marrow dosimetry for radioimmunotherapy: Theoretical considerations. *J Nucl Med* 1993;34:689-694.
14. Verel I, Visser GW, van Dongen GA. The promise of immuno-PET in radioimmunotherapy. *J Nucl Med* 2005;46 Suppl 1:164S-171S.
15. Dijkers EC, Lub-de Hooge MN, Kosterink JG, Jager PL, Brouwers AH, Perk LR, et al. Characterization of  $^{89}\text{Zr}$ -trastuzumab for clinical HER2 immunoPET imaging. *J Clin Oncol* 2007;25:3508.
16. Perik PJ, Lub-de Hooge MN, Gietema JA, van der Graaf WT, de Korte MA, Jonkman S, et al. Indium-111-labeled trastuzumab scintigraphy in patients with human epidermal growth factor receptor 2-positive metastatic breast cancer. *J Clin Oncol* 2006;24:2276-2282.
17. Nagengast WB, De Vries EG, Hospers GA, Mulder NH, de Jong JR, Hollema H, et al. In vivo VEGF imaging with radiolabeled bevacizumab in a human ovarian tumor xenograft. *J Nucl Med* 2007;48:1313-1319.
18. Aerts HJLW, Dubois L, Perk LR, Vermaelen P, van Dongen GAMS, Wouters BG, et al. Disparity between in vivo EGFR expression and zirconium-89-labeled cetuximab uptake assessed by PET. *J Nucl Med* 2009;50:123-131.
19. Perk LR, Visser OJ, Stigter-Van Walsum M, Vosjan MJ, Visser GW, Zijlstra JM, et al. Preparation and evaluation of  $^{89}\text{Zr}$ -Zevalin for monitoring  $^{90}\text{Y}$ -Zevalin biodistribution with positron emission tomography. *Eur J Nucl Med Mol Imaging* 2006;33:1337-1345.